



Experimental And Numerical Studies Of Structural Behavior Of Segmental Arch Beam

Asaad hamdan maryoosh ¹

asaad.hamdanmaryoosh@gmail.com

1. Master's degree in Civil Engineering, Ministry of Education, Baghdad, Iraq.

Shaima Sabri Ali ²

shaimasabri@yahoo.com

2 Lecturer, Civil Engineering Department, Ministry of Education, Baghdad, Iraq.

Dr. Waleed Awad Waryosh ³

waleedwaryosh@uomustansiriyah.edu.iq

3 Assistant Professor, Civil Engineering Department, Mustansiriyah University, Baghdad, Iraq.

ABSTRACT

This investigation aims to study the structural behavior of reinforced concrete arches. To achieve this aim; the experimental and numerical analyses were conducted. Five reinforced concrete arches prepared in the lab and tested under static loading at mid-span of the arches. The cross-section of these arches was T-section. The parametric studies were also accomplished to emulate the influence of differences in segmental configuration, number of segments and the types of the joints on the real structural response of reinforced concrete arches. Also, the numerical analysis was carried out by using a commercial finite element program that is ANSYS v.18.2. The numerical results compared with the experimental measurements. It is found that the peak percentage difference between numerical and experimental results not greater than 16%, and hence, good agreement achieved between them. The main results of this investigation that is the segmental configuration of concrete has active effects on the strength capacity of the reinforced concrete arch and on the deflection. Additionally, the ultimate load of the arches that are consist of the joints decreased by 23% to 57% compared with the reference arch.

Keywords:

Reinforced Concrete Arches, segmental configuration, types of joint.

Introduction

Arches are curving structural elements that are utilized in a variety of engineering building applications [1]. Hutchinson [2] covered segmental precast arch analysis and design in 2000. The models were constructed using the finite elements technique, which applied particular loading until the arches failed.

The segmental arch is fast, adaptable, and cost-effective when employed in transportation projects, according to the analysis's findings.

Radić et al. [3] examined a variety of building techniques that were modified to build reinforced concrete arch bridges in 2004. The building of several bridges significantly enhanced the development of free cantilever construction techniques for big and long concrete arch bridges, according to the

evaluated construction methods. Tang et al. (2005). [4], examined the concrete arch structural section damage as well as the mode and process of collapse using numerical methods.

Zhou et al. [5] investigated the segmental arch bridge's shear strength in 2005. The investigated parameters included different joint configurations, namely flat joints and single-keyed joints, as well as multiple-keyed joints for both dry and epoxy-bonded conditions under varying epoxy quantities and stress levels. When the experimental results were compared with the shear design equations and criteria specified in AASHTO and other design standards, it was observed that these equations frequently underestimated the shear capacity developed at single- and multiple-keyed joints by up to approximately 40%, while they tended to overestimate the shear strength in the case of dry joints. In addition, Zhang et al. [6] examined an existing concrete arch bridge that had been in service for about 28 years to evaluate its structural behavior and overall performance. The load with strain and displacements was assessed using numerical analysis and experimental testing. Investigations revealed that the final strength and failure mode were significantly impacted by the first fractures, the primary corrosion of the reinforcement, and the modification of the arch axial line form. Zheng [7] reviewed a variety of Chinese arch bridges made of concrete and steel tubes filled with concrete in 2007. The information gathered about the arch sections was categorized according to the materials used in their construction, including concrete, stone, steel, and hollow steel sections filled with concrete. There were about 151 concrete arch bridges and around 130 composite bridges with a span of more than 100 meters, according to the number of bridges. The span of the bridge, the structural system, and the construction methods are the primary characteristics used to gather all data and analyze it statistically. The conclusions drawn from the study are that arch bridge designers must consider cost while designing a bridge.

Kim et al. [8] examined the joints between precast post-tensioned segments using a numerical technique in 2007. A computer software called RCAHEST, a nonlinear finite element analysis program for examining reinforced concrete structures, solved the model as nonlinearity material. When building the model, the slide that occurred at the joint surfaces was taken into consideration. Gao et al. [9] suggested using CFRP that has been deformed and reinforced for arch bridge suspenders in 2013. Because CFRP has superior corrosion resistance, it was suggested as a treatment. In 2014, Ali and Hamza [10] investigated the performance of a reinforced concrete arch with openings at several points, including the arch's top and its sides, which were reinforced with CFRP. Gao and Zhao [11] investigated the use of CFRP to treat steel bridge collapses caused by fatigue and environmental impacts in 2015.

The concrete arch's segmental structure, number of segments, and joint type are the criteria that are taken into consideration in this job. Examined are the effects of segmental arrangement, segment count, and joint types on the behavior of reinforced concrete arches during experimental testing.

2. Experimental program

All specimens were prepared and tested in construction and structural labs for civil engineering department of Al-Mustansiriyah university. The details of experimental program can be drawn in the following sections:





2.1 Mechanical properties of materials

The goal of this study is to assess joint behavior in segmental arch designs and offer suggestions for achieving appropriate performance. When cubes, cylinders, and prisms are examined, the average of three specimens is used at 28 days. Ordinary Portland cement, which has a maximum size of 4.75 mm for fine aggregate and 10 mm for coarse aggregate, is the type of cement used. Using the same concrete mix for all beams as indicated in tables [1] and [2], the experimental program in this study entails casting and testing four reinforced concrete arches with dimensions of (300,75,300,150,500, and 2100) mm (width of flange, thickness of flange, height of web, width of web, clear height of concrete arch, and span of concrete arch).

Table 1: Mix design based on the compressive strength of concrete

Material	cement	Sand	Gravel	water
	kg/m ³	kg/m ³	kg/m ³	Liter/m ³
Weight	400	600	1200	180

Table 2: Arch sampling

Arch number	Arch name	Type of Arch	
1	AR1	Reference Arch (without segment)	
2	AR9	Segment Arch (three segment)	
3	AR10	Segment Arch (three segment)	
4	AR11	Segment Arch (two segment)	
5	AR12	Segment Arch (two segment)	

Three specimens were tested for each reinforcing bar diameter used in the top reinforcement, bottom reinforcement, and stirrups of the concrete arches in order to determine the yield strength, ultimate tensile strength, and Young’s modulus under static loading conditions. The corresponding experimental results are summarized in Table (3).

Table 3: Properties of steel reinforcement

Nominal Diameter(mm)	Yield tensile strength f _y (MPa)	Ultimate tensile strength f _u (MPa)	E _s (MPa)
12	410	610	200000
10	405	596	200000

2.2. Supports and loadings conditions

The boundary conditions for each specimen are set to fixed at the ends. The specimens are set up with an arch span of 2100 mm, and their top faces are loaded with a central point load. As seen in Figure (1), a solid rod was used to distribute the applied stress along the specimen's width (line loading). As control, the was to the specimens increasing



load
load
applied
in

increments until they failed.

Figure 1: Applied loading setup

2.3 Test methodology

Five reinforced concrete arches were tested in all. Figure (2) displays the profile, arrangement, and details of the arches. Based on the kind of concrete, segmental arches, and strip spaces, the examples are divided into five categories. All specimens have arches that are 500 mm high at the bottom face and 2100 mm long. The web and flange of the arch examples have the same compressive strength (f_c') of 25 MPa, with stirrups measuring 10 mm in diameter and 150 mm from center to center. The concrete and reinforcement in every specimen—aside from the control AR1—ended at the joints, leaving the CFRP at the junctions as the sole connection between the segmental parts. The parameters of SikaWrap, 300 C/60, are 0.166 mm in thickness and 9300 mm in width. Its modulus of elasticity is 230000 MPa, its elongation is 1.5%, and its tensile strength is 3900 MPa.

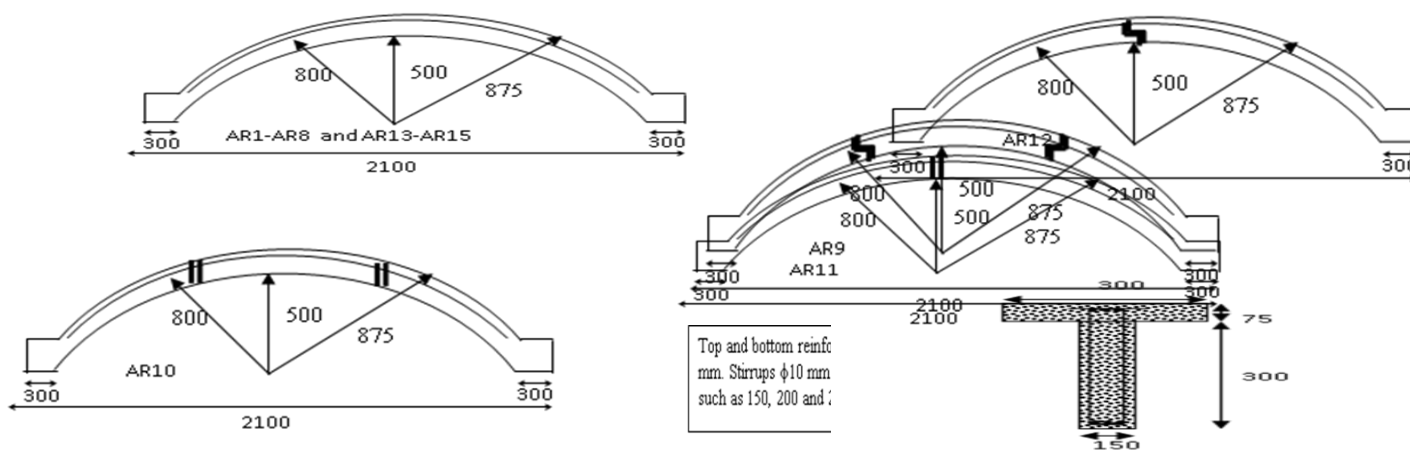


Figure 2: Arches configuration and geometry, all dimensions in mm

2.4 Tests results

Table 2 lists five variations in reinforced concrete arches that were exposed to static loads until they failed. The specimens before and after the test are shown in Figures (3) to (7). For specimen AR1, the mode of failure at the joints is flexural; for other specimens, it is shear. Figures 8 and 9 depict the whole behaviour of the load-deflections at the arch centre and at a quarter of the arch span, respectively. Up to the initial crack loadings, all specimens show linear behaviour. After that, the concrete becomes weaker as applied loading increases until failure, resulting in nonlinear behaviour and a curve that is orientated towards the horizontal axis. Table 3 provides a summary of the test results.



Figure 3: Specimen AR1 before and after test with cracks propagations



Figure 4: Specimen AR9 before and after test with cracks propagations



Figure 5: Specimen AR10 before and after test with cracks propagations



Figure 6: Specimen AR11 before and after test with cracks propagations



Figure 7: Specimen AR12 before and after test with cracks propagations

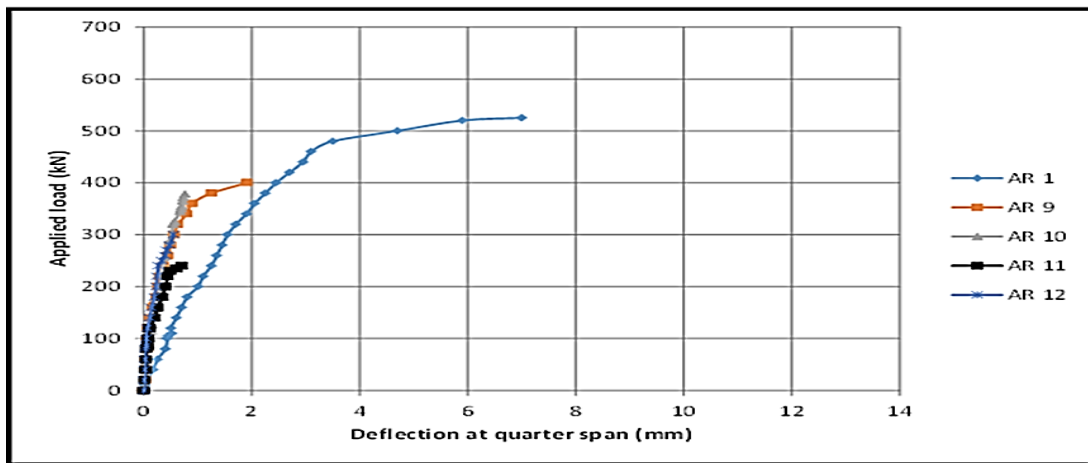


Figure 8: Load- deflection behavior for all specimens at quarter of span

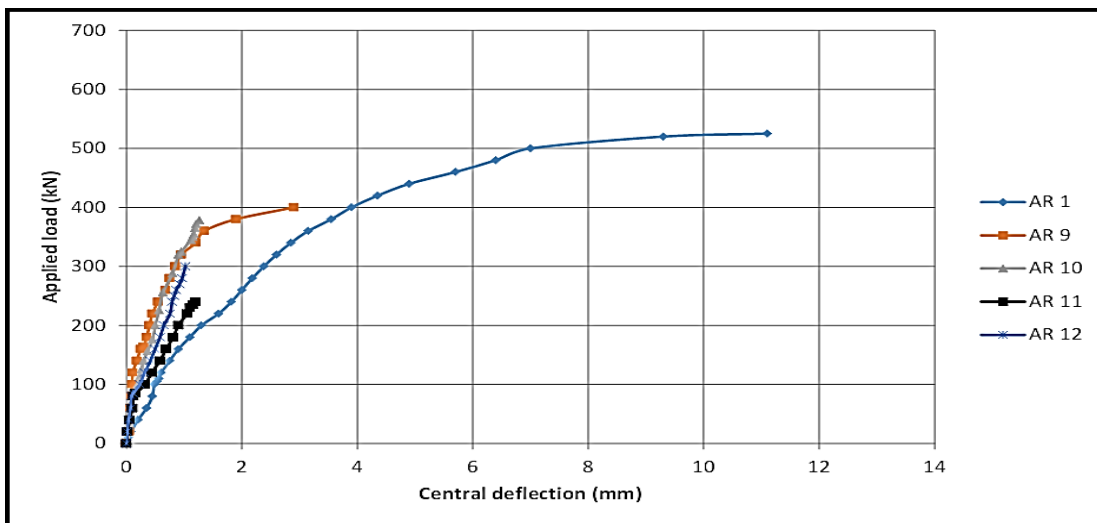


Figure 9: Load- deflection behavior for all specimens at center of span

Table 3: tests results summarized for all specimens

Specimen mark	First cracks load P_c (kN)	Ultimate load P_u (kN)	% of change related to control specimen	Deflection at ultimate load (mm)	
				Quarter span	Central
AR 1	105	525	0	7.00	11.10
AR 9	164	400	-23.81	1.92	2.90
AR 10	120	370	-29.52	0.76	1.27
AR 11	85	230	-56.19	0.71	1.20
AR12	120	300	-42.85	0.55	1.10

3. Discussions of experimental results

The control specimen gave strength load capacity more than other specimens because casted at without joints. In case of specimen (AR9), the ultimate load capacity is (400 kN) with maximum deflection at failure is (2.90 and 1.92 mm) at center and quarter of the arch specimen span respectively. The load capacity reduced by (23.81%) in which the mechanical properties are same for specimen (AR1) but different that the presence of stepped two joints at the one-third of the span. The joints are warped by CFRP to re-strengthening the arch specimen.

The maximum deflection at the center and quarter of the arch span are small as compared with the other specimens because of shear failure at the joints as shown in fig. (8) and (9). In case of specimen (AR10), the ultimate load capacity is (370 kN) with maximum deflection at failure is (1.27 and 0.76 mm) at center and quarter of the arch specimen span respectively. The load capacity reduced by (29.52%) in which the mechanical properties are same as for specimen (AR1) and (7.5%) as compared with specimen (AR9), the specimen (AR10) have a straight two joints at the one-third of the span. The joints are warped by CFRP to the arch specimen. The maximum deflection at the center and quarter of the arch span are small as compared with the other specimens of this group (G3) because of shear failure at the joints.

The specimen (AR11), the ultimate load capacity is (230 kN) with maximum deflection at failure is (1.20 and 0.71 mm) at center and quarter of the arch specimen span respectively. The load capacity reduced by (56.19%) in which the mechanical properties are same for specimen (AR1) and (37.83%) as compared with specimen (AR10), the specimen (AR11) have a straight joint at the center of the span. The joints are warped by CFRP to the arch specimen. The maximum deflection at the center and quarter of the arch span are small as compared with the other specimens because of shear failure at the joints.

While, in case of specimen (AR12), the ultimate load capacity is (300 kN) with maximum deflection at failure is (1.10 and 0.55 mm) at center and quarter of the arch specimen span respectively. The load capacity reduced by (42.85%) and (25%) as compare with the specimens (AR1) and (AR9) respectively. The maximum deflection at the center and quarter of the arch span are small as compared with the other specimens because of shear failure at the joints.

4. Numerical Results

All recorded results from experimental investigation are compared with the numerical results by finite elements analysis. Figures (10) represent the arch model with central CFRP. Figures (11) show the arch model with double CFRP that wrapped around the joints at the one-third of the arch.

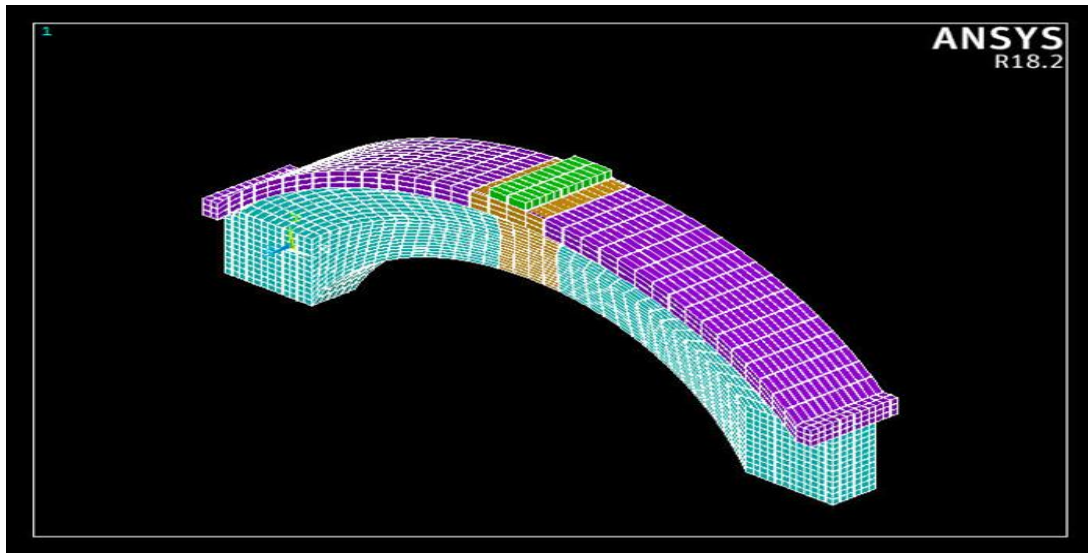


Figure 10: Finite elements mesh of the model with CFRP -3D- models AR11 and AR12 straight and stepped Joint

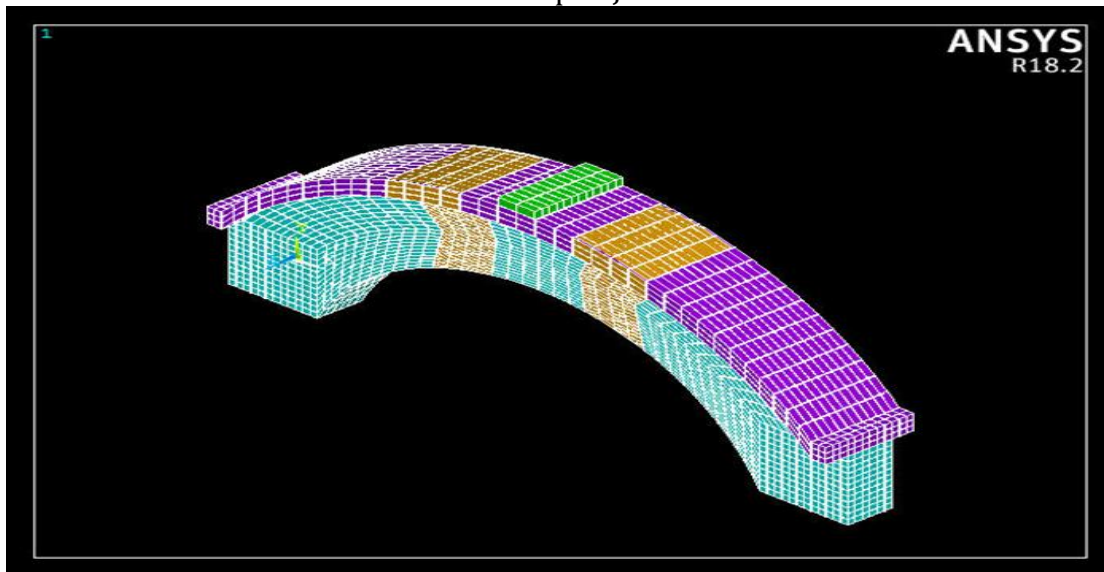


Figure 11: Finite elements mesh of the model with CFRP -3D- for models AR9 and AR10 straight and stepped Joints

The load-deflection behavior shown in the Figure (12) represent the model AR1 same in behavior as experimental test. The numerical solution gave approximate results at different stages up to failure stage.

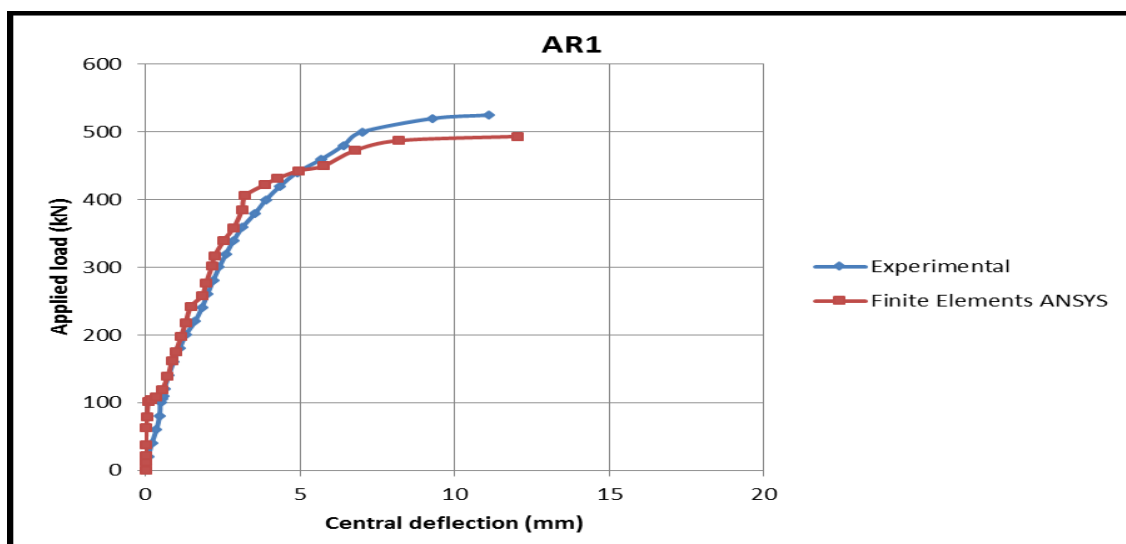


Figure 12: Load-deflection behavior of specimen AR1 as experimental and finite elements comparison. The applied loads in finite elements same as that resulted from experimental tests but the model fail at (94%) from the load as recorded in experimental test. The deflection values within elastic range in case of finite elements less than experimental test result due to rigid connections between nodes of the model. The maximum percentage different between numerical and experimental results was (8.21%) AR1. The stiffness of the model reduces after inflection point because of increase in deflection of the model.

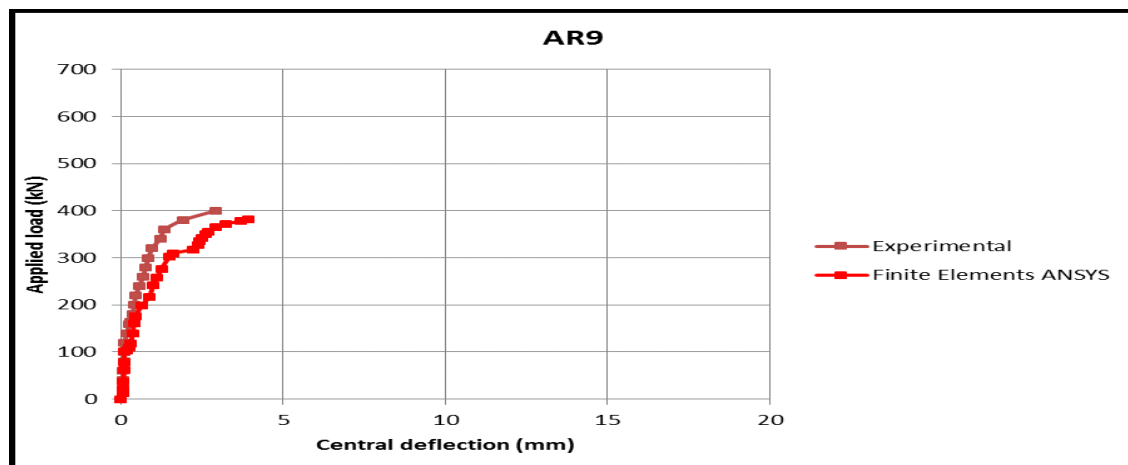


Figure 13: Load-deflection behavior of specimen AR9 as experimental and finite elements comparison

In case of models AR9 fig. (13), the load capacity in finite elements reach (93%) from the load capacity of experimental test with deflection at failure stage (2.9 mm) compared with the test (4.1 mm) The highest percentage different recorded between numerical and experimental deflection was (34.28%) AR9.

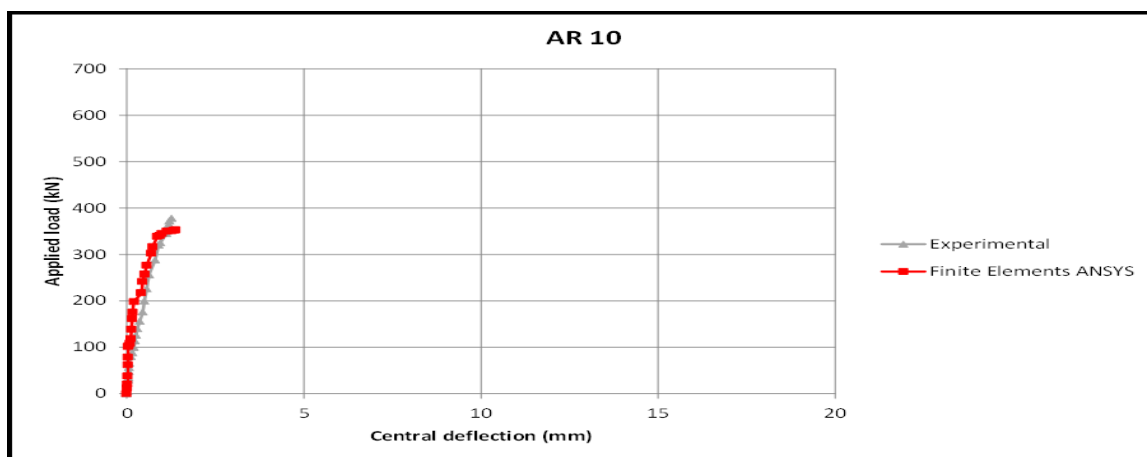


Figure 14: Load-deflection behavior of specimen AR10 as experimental and finite elements comparison

The model AR10 as shown in Figure (14), the finite elements analysis gave the ultimate load strength (94%) from the strength capacity of the concrete arch in experimental test. The maximum percentage different between numerical and experimental results was (19.85%) AR10.

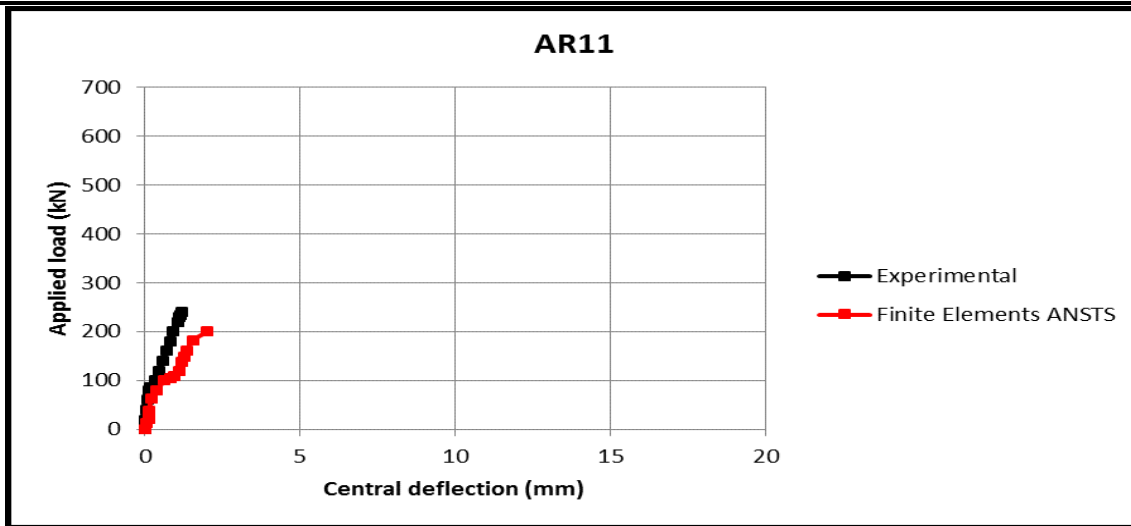


Figure 15: Load-deflection behavior of specimen AR11 as experimental and finite elements comparison

In case of model AR11 fig. (15) the finite elements model that built to check out the experimental test taking into account the same mechanical properties and load capacity reached up to (85%).while The peak percentage different between numerical and experimental deflection was (54.54%).

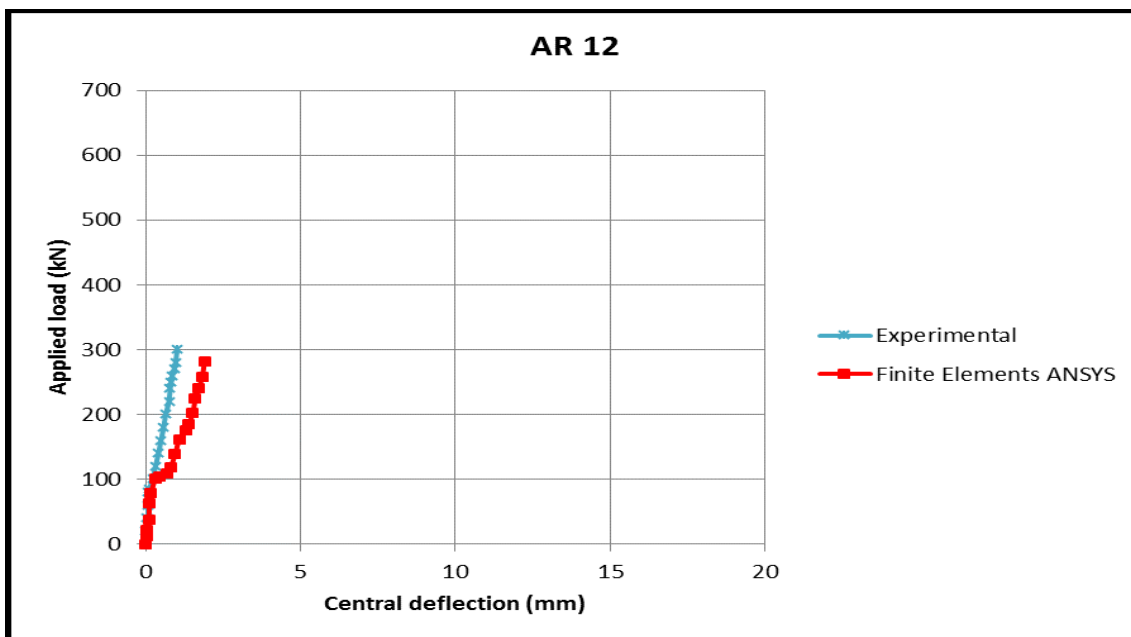


Figure 16: Load-Deflection Behavior of Specimen AR12 as Experimental and finite Elements Comparison

Model AR12 the finite elements model the load capacity reached up to (94%). The highest percentage different between numerical and experimental results was (58.06%). for specimen (AR9, AR11, AR12) recorded high ratio of deflection because of its joint and segments. While AR10 less than of there specimens. The model performance like the experimental behavior in which there is inflection point in finite elements analysis but still the curve rise up to failure.

5. Parametric Study

The load-deflection behavior shown in the Figure (17) represent the model AR1 in case of the same model but the compressive strength of the web is (50 MPa), the ultimate load reached to (623 kN) and the maximum deflection was (6.90 mm). It is noticed the load capacity increased (18.67%) when increased the compressive strength that was (50) Mpa and the maximum percentage different between numerical for parametric study for increase f'_c (50) Mpa for web results was (46.67%) AR1 at ultimate load.

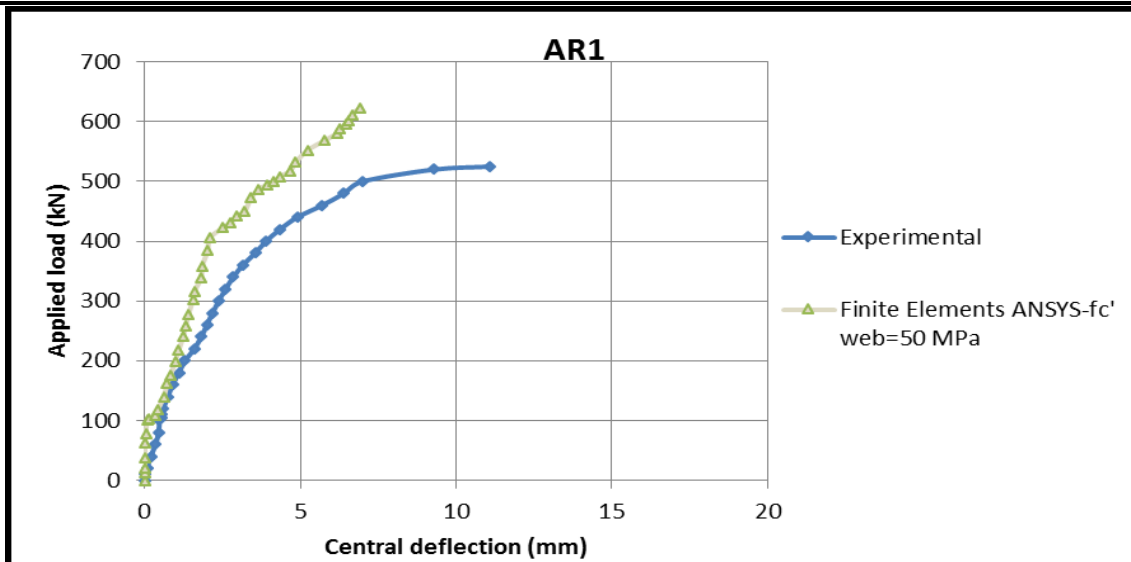


Figure 17: Load-deflection behavior of specimen AR1 as experimental and finite elements comparison-change web compressive strength to 50 MPa

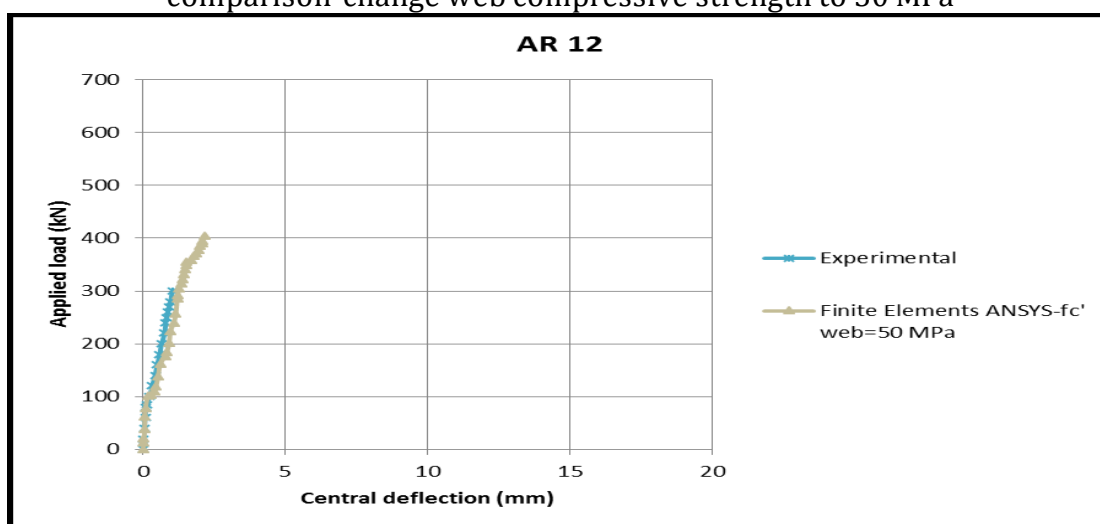


Figure 18: Load-deflection behavior of specimen AR12 as experimental and finite elements comparison-change web compressive strength to 50 MPa

For the models AR12 as shown in Figure (5.33), the strength capacity increased as the compressive strength of the web become (50 MPa) and the deflections compared with the reference load decreased. The increase in web compressive strength make the modulus of elasticity increase and the elastic deformation of the concrete enhanced so that the deflection for same load of experimental test become less and the load capacity of the concrete arch become more (395 kN) while in experimental test (300 kN), the increase percentage in load capacity is (31.67%). the maximum percentage different between numerical for parametric study for increase f'_c (50) Mpa for web results was (53.33%) AR12 at ultimate load.

Presence of main reinforcements in the flange is not considered in the design of reinforced concrete arches that tests in laboratory. In case of models AR9 as shown in Figure (19), The parametric study for this model add main reinforcements at the top flange of the concrete arch and kept all other parameters same. The load capacity in the presence of reinforcements increase up to (565 kN) with increase percentage as compared with the load capacity from test (41.25%).

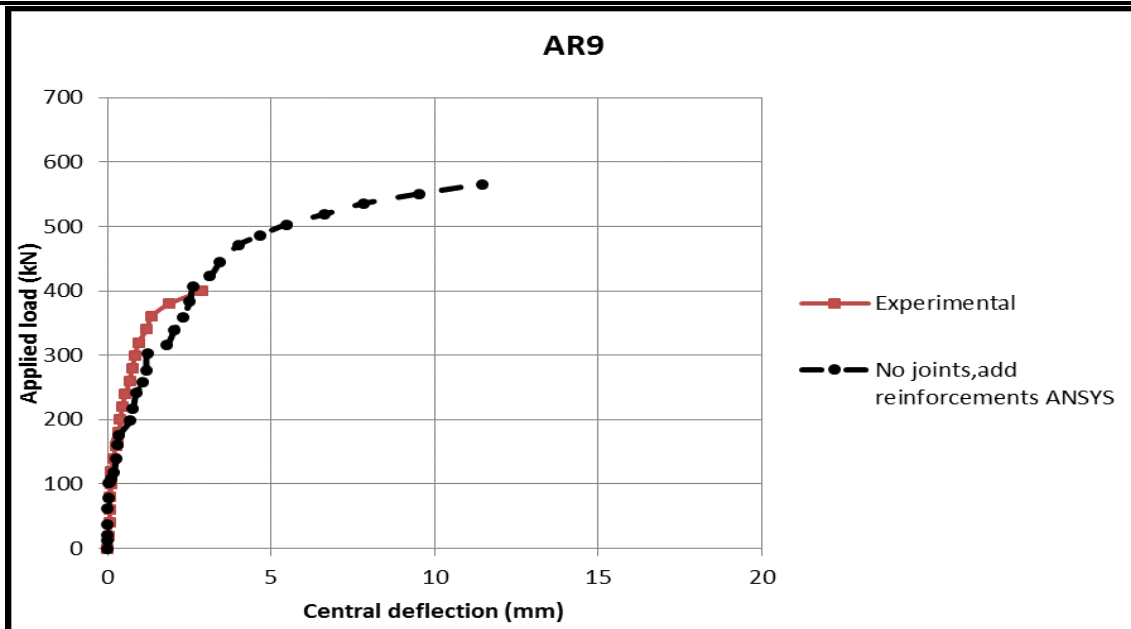


Figure 19: Load-deflection behavior of specimen AR9 as experimental and finite elements comparison-add flange reinforcements

In case of model AR11 as shown in Figure (20), same amounts of reinforcements are adopted and at the joints locations the bars are continuous. The strength capacity decreased and the deflections compared with the reference load increased in presence of flange reinforcements. The presence of the reinforcement rebar's lead to make the concrete flange more ductile and gave more strength resistance to the applied load and the model become more moment resistance. The increase in load resistance is around (178%) as compared with the experimental test this is because of steel reinforcement was continuous with joint.

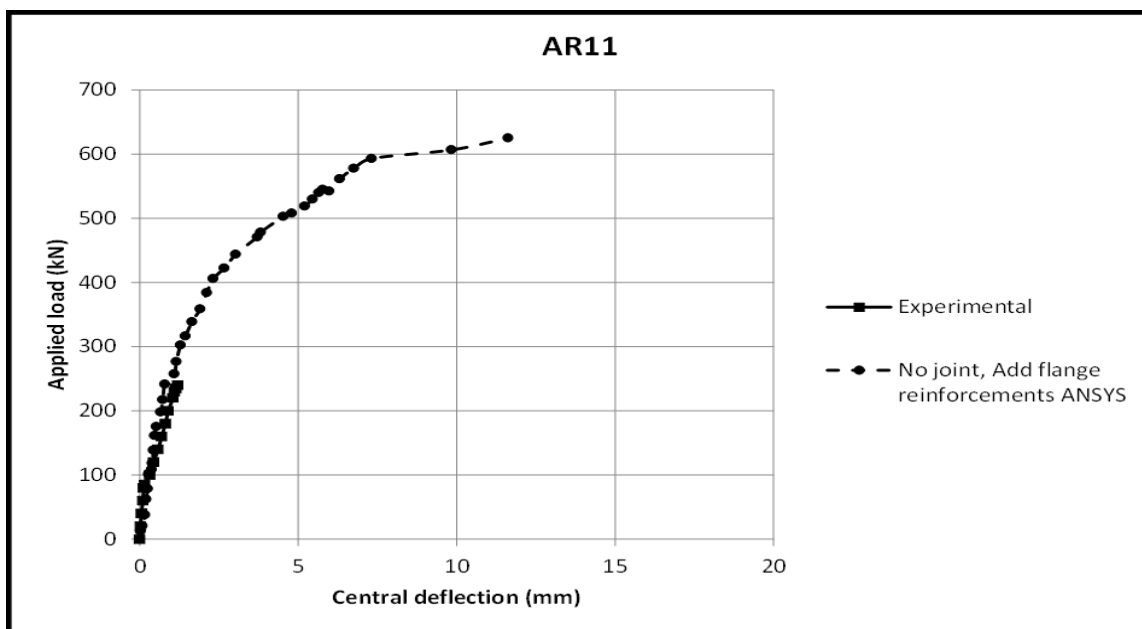


Figure 20: Load-deflection behavior of specimen AR11 as experimental and finite elements comparison-add flange reinforcements.

6. Conclusions

The following are the observations and conclusions drawn from the test findings:

1. Compared to other specimens, the control reinforced concrete arch AR1 provided a higher strength capability. This is due to the continuous reinforcing and a continuous cast for every portion at once.
2. Because there was less shear stress and more shear friction (chair key), the steeped key provided more resistance and strength capacity than the straight key. Because each segment rested on

- another, increasing the specimen's resistance, steeped keys produced less deflections than chair keys. In comparison to the specimen with a straight key (AR10), the specimen with a chair key (AR9) produced more strength (8.11%) and less deflection (14.68%) at ultimate load. Additionally, the segment arch joints that are deformed by CFRP were able to re-strengthen some of the arch specimens with keys.
3. The maximum deflection at the center and quarter of the arch span are small values as compared with the other specimens. Specimen control change (AR1) the web compressive strength to (75 MPa) gave increase in load capacity (18.67%) and decrease in deflection (57.65%) for same load. Specimen (AR11) with joint at the middle of the arch and add reinforcements in the flange gave increase in load capacity (178%) and decrease in deflection (33.17%) for same load. Specimen (AR12) with chair key at the middle change the web compressive strength to (50 MPa) gave increase in load capacity (31.67%) and the maximum percentage different between numerical for parametric study was (53.33%) AR12 at ultimate load. Specimen (AR9) with chair key joints and add reinforcements in the flange gave increase in load capacity (41.25%) and decrease in deflection (18.24%) for same load.
 4. In experimental tests segments arches failed in shear mode at the joints that warped by CFRP. In experimental tests the specimens with chair key joints failed in both shear and flexural. The location of joint at the center gave strength capacity less than that at the one third of the span. Segments arches have deflection and strain at the mid span and at quarter for central joint are greater than the other joint location. In experimental tests the flexural strength capacity of the chair key joint gave more resistance and less deflection than the straight joint.
 5. The results of the numerical models are shown close with test results with some percentage not greater than in maximum (16%) from the ultimate load capacity in experimental. For specimens AR1, AR9, AR10, AR11 and AR12 (6.28, 7.25, 6.41, 15.96 and 6.18).

References

1. Robertson, D.S.: Greek and Roman Architecture, 2nd Edition, Cambridge 1943, p.231
2. David Hutchinson (2000). "*Application and design of segmental precast arches*", The Reinforced Earth Company, Vol. 99, pp. 1-9.
3. Radić, J., Šavor, Z. and Puž, G.(2003). "*Construction methods for reinforced concrete arch bridges*".
4. Tang, X.S., Zhang, J.R., Li, C.X., Xu, F.H. and Pan, J. (2005). "*Damage analysis and numerical simulation for failure process of a reinforced concrete arch structure*", Computers & structures, Vol. 83, No. 31-32, pp. 2609-2631.
5. Xiangming Zhou (2005). "*Shear strength of joints in precast concrete segmental bridges*", ACI Structural Journal/January-February, pp. 3-11.
6. Zhang, J.R., Li, C.X., Wang, L., Xu, F.H. and Yu, X.M.(2006). "*Experiment and analysis on the ultimate strength of existing reinforced concrete arch rib*", Engineering Mechanics, Vol.23, No.12, pp. 136-142.
7. Zheng, L.I., Lu-kuan, Q.I., Jian-yong, S.O.N.G. and Zu-sheng, L.I.U. (2007). "*Modeling with Parameters and Eigenvalue Buckling Analysis of Reinforced Concrete Arch Bridges*", Journal of Highway and Transportation Research and Development, Vol. 4, pp. 025.
8. Tae-Hoon Kim (2007). "*Numerical study on the joints between precast post-tensioned segments*", International Journal of Concrete Structures and Materials, Vol.19, No.1E, pp.03-09.
9. Gao, J., Chen, C.M., Winistörfer, A. and Meier, U. (2013). "*Proposal for the application of carbon fiber reinforced polymers (CFRP) for suspenders of arch bridges in China*". Proceedings of SMAR.
10. Ali, A.Y. and Hamza, B.A. (2015). "*Finite element analysis of RC Arches with openings strengthened by CFRP laminates*", In *COMPLAS XIII: proceedings of the XIII International Conference on Computational Plasticity: fundamentals and applications*, pp. 495-506.
11. Gao J., Zhao B.(2015). "*Application of CFRP Suspenders for Through and Half-through Arch Bridges*", Proceedings of the 2015 4th International Conference on Sustainable Energy and Environmental Engineering, Advances in Engineering Research.

